New Phytologist

Research

Ectomycorrhizal fungi integrate nitrogen mobilisation and mineral weathering in boreal forest soil

Shahid Mahmood[1], Zaenab Fahad[1], Emile B. Bolou-Bi[2], Katharine King[1], Stephan J. Köhler[3], Kevin Bishop[3], Alf Ekblad[4] and Roger D. Finlay[1]

[1]Department of Forest Mycology and Plant Pathology, Uppsala BioCenter, Swedish University of Agricultural Sciences, Box 7026, SE-750 07, Uppsala, Sweden; [2]UFR des Sciences de la Terre et des Ressources Minières, Département des Sciences du sol, Université Felix Houphouët-Boigny, 22 BP 582, Abidjan, Côte d'Ivoire; [3]Department of Aquatic Sciences and Assessment, Soil-Water-Environment Center, Swedish University of Agricultural Sciences, Box 7050, SE-750 07, Uppsala, Sweden; [4]School of Science and Technology, Örebro University, SE-701 82, Örebro, Sweden

Author for correspondence:
Shahid Mahmood
Email: shahid.mahmood@slu.se

Received: *9 June 2023*
Accepted: *24 August 2023*

New Phytologist (2024) **242:** 1545–1560
doi: 10.1111/nph.19260

Key words: boreal forests, carbon allocation, carbon sequestration, ectomycorrhizal fungi, mineral weathering, nitrogen mobilisation, organic matter, podzol horizons.

Summary

- Tree growth in boreal forests is driven by ectomycorrhizal fungal mobilisation of organic nitrogen and mineral nutrients in soils with discrete organic and mineral horizons. However, there are no studies of how ectomycorrhizal mineral weathering and organic nitrogen mobilisation processes are integrated across the soil profile.
- We studied effects of organic matter (OM) availability on ectomycorrhizal functioning by altering the proportions of natural organic and mineral soil in reconstructed podzol profiles containing *Pinus sylvestris* plants, using $^{13}CO_2$ pulse labelling, patterns of naturally occurring stable isotopes (^{26}Mg and ^{15}N) and high-throughput DNA sequencing of fungal amplicons.
- Reduction in OM resulted in nitrogen limitation of plant growth and decreased allocation of photosynthetically derived carbon and mycelial growth in mineral horizons. Fractionation patterns of ^{26}Mg indicated that magnesium mobilisation and uptake occurred primarily in the deeper mineral horizon and was driven by carbon allocation to ectomycorrhizal mycelium. In this horizon, relative abundance of ectomycorrhizal fungi, carbon allocation and base cation mobilisation all increased with increased OM availability.
- Allocation of carbon through ectomycorrhizal fungi integrates organic nitrogen mobilisation and mineral weathering across soil horizons, improving the efficiency of plant nutrient acquisition. Our findings have fundamental implications for sustainable forest management and belowground carbon sequestration.

Introduction

Forests are large and persistent sinks for atmospheric carbon dioxide (CO_2; Pan *et al.*, 2011) and large-scale afforestation and reforestation have been suggested as methods for mitigating climate change through carbon sequestration (Law *et al.*, 2018; Nave *et al.*, 2018; Bastin *et al.*, 2019; Pugh *et al.*, 2019; Domke *et al.*, 2020). However, intensification of forestry (Kastner *et al.*, 2021), including removal of organic residues for bioenergy (Daiogloua *et al.*, 2019), has led to concern about sustainability of base-cation supply (Achat *et al.*, 2018; Akselsson *et al.*, 2019), and better understanding of the ecological and biogeochemical consequences of different management practices is needed (Palmer, 2021).

In forests, symbiotic and decomposer fungi play pivotal roles in sequestration and release of carbon (C; Jones *et al.*, 2009; Clemmensen *et al.*, 2013). The flow of photosynthetically derived C through ectomycorrhizal fungi is important in mobilising nitrogen (N) from organic matter (OM), as well as weathering of mineral substrates (Finlay *et al.*, 2020). There is conflicting evidence concerning whether mobilisation of organic N is linked to net mobilisation or net sequestration of C (Averill *et al.*, 2014; Zak *et al.*, 2019; Clemmensen *et al.*, 2021; Lindahl *et al.*, 2021), but in an evolutionary perspective, there is consensus that ectomycorrhizal symbiosis has intensified mineral weathering and driven drawdown of global CO_2 by enhancing land to ocean calcium (Ca) export and C sequestration into marine carbonates (Quirk *et al.*, 2012, 2014). Enhanced weathering of added silicate rocks has been suggested as a method to mitigate climate change by sequestering C from the atmosphere (Beerling *et al.*, 2020; Kantzas *et al.*, 2022).

In boreal forests, tree growth is driven by mobilisation of (predominantly) organic N and mineral nutrients from vertically stratified soils consisting of an organic (O) horizon overlying an eluvial (E) and a deeper illuvial (B) mineral horizon. Decomposition and weathering in these distinct, but contiguous, soil horizons have been studied, in detail, within essentially separate research traditions by different groups of researchers. This has

hindered mechanistic understanding of how the processes of N mobilisation and biological mineral weathering influence each other, and how these processes are related to patterns of C allocation.

Many studies of ectomycorrhizal fungi have been conducted in the upper, organic horizon, concentrating on fungal mobilisation of nutrients and diversity of fungal communities (Clemmensen *et al.*, 2013, 2015, 2021; Näsholm *et al.*, 2013; Lindahl *et al.*, 2021). Extensive use has been made of stable isotopes of N (Högberg, 1997; Näsholm *et al.*, 2013) to improve understanding of N acquisition and cycling and there is now a broad consensus that, during evolution from saprotrophic ancestors, certain ectomycorrhizal fungi have retained the genetic potential to mobilise N from recalcitrant OM (Lindahl & Tunlid, 2015). Comparatively, few studies have been conducted in the deeper mineral soil horizons, although there are reports that two thirds of mycorrhizal root tips and half of the ectomycorrhizal taxa (Rosling *et al.*, 2003), and half or more of the mycelial biomass (Ekblad *et al.*, 2013) occur in the mineral horizons. Since it was proposed that ectomycorrhizal fungi might weather mineral substrates (Jongmans *et al.*, 1997), there has been increased interest in biological weathering, in particular the role of ectomycorrhizal fungi. The subject has been reviewed from an evolutionary perspective and regarding different spatial scales (Leake & Read, 2017; Finlay *et al.*, 2020). Allocation of C to fungal mycelia results in weathering leading to mobilisation of the base cations and phosphorus (P) essential for plant growth, but existing studies of fungal weathering (see Finlay *et al.*, 2020) are mostly based on individual species inoculated into laboratory microcosms containing artificial substrates. Little mechanistic information is available from natural forest soils, with fungal communities identified *in situ*.

The aim of the present study was to investigate the effects of changes in OM availability in the surface horizon on: (1) plant and fungal mycelial biomass, (2) spatial allocation patterns of plant assimilated C, (3) fungal community composition and the relative abundance and spatial distribution of different functional fungal guilds in soil, and (4) mobilisation and uptake of base cations, P and N. We used microcosms containing different proportions of naturally occurring organic and mineral layers from a boreal forest podzol, creating a gradient of OM availability (Fig. 1a). *Pinus sylvestris* plants were grown in the reconstructed podzol profiles for 14 months. Plants were pulse labelled with $^{13}CO_2$ to study C allocation to different soil horizons and mobilisation of base cations was studied by examining patterns of fractionation of naturally occurring stable isotopes of magnesium (Mg). The composition of fungal communities in different soil horizons was studied using high-throughput DNA sequencing. We hypothesized (1) that the higher availability of OM would increase the amount of N mobilised by ectomycorrhizal fungi and supplied to their plant hosts, and (2) that this would increase plant growth and the supply of photosynthetically derived C allocated to ectomycorrhizal fungi. We further hypothesized (3) that increased allocation of C to ectomycorrhizal fungi would improve their ability to mobilise base cations and P from mineral substrates. Based on evidence that ectomycorrhizal fungi appear to discriminate against uptake of heavy ^{26}Mg (Fahad *et al.*, 2016), we expected (4) that greater uptake of Mg would lead to enrichment of $\delta^{26}Mg$ signatures in soil solution in environments where ectomycorrhizal fungi proliferate, supported by C directly from their host plants.

Materials and Methods

Plant and soil preparation

Pinus sylvestris L. seeds were surface sterilised with 33% hydrogen peroxide for 30 min, rinsed thoroughly with milliQ water, air dried and dispersed into a plant propagator (30 × 20 × 20 cm) filled with 2 l of nonsterile vermiculite. The propagators were incubated in a phytotron with a 250 μmol m^{-2} s^{-1} photosynthetically active radiation (PAR) 18 h : 6 h, light : dark cycle and day : night temperature of 18°C : 16°C. The germinating seedlings were incubated under these parameters for *c.* 4 months before use. The seedlings were irrigated weekly with deionised water.

Soil was collected from the organic (O), eluvial (E) and illuvial (B) horizons of a podzol under a well-documented forest at Ivantjärnsheden, Jädraås, central Sweden (60°49′N, 16°30′E, altitude 185 m), located at the border between the Swedish boreal and boreo-nemoral zones (Persson, 1980; Mielke *et al.*, 2022). The forest consists of a homogenous, evenly aged (160 yr) stand of *Pinus sylvestris* L. with a few scattered *Picea abies* (L.) Karst. The understorey consists of the ericaceous dwarf shrubs *Vaccinium vitis-idaea* L. and *Calluna vulgaris* (L.) Hull, with a lower cover of *Empetrum nigrum* L. and *Vaccinium myrtillus* L. and feather moss *Pleurozium schreberi* (Brid.) Mitt. (Bråkenhielm & Persson, 1980). The soil profile consists of a glacifluvial sand podzol, a mor layer (pH 3.0) and a pale eluvial horizon overlying a rust-red illuvial horizon of the mineral soil (pH 4.4–4.8; Bringmark, 1980). The bedrock is composed of granites, sediments and volcanic rocks, which are widespread in Fennoscandia. Organic and mineral horizon soils were homogenised using 5 and 3 mm mesh sieves, respectively. Freshly fallen tree litter, stones, roots and lichens were all removed. Details of the elemental composition of O, E and B horizon soils (Marupakula *et al.*, 2017) are given in Supporting Information Table S1.

Two-compartment mesh bag preparation

To enable harvesting of clean mycelium, free of adhering soil particles (for analysis of elemental and isotopic composition), a two-compartment mesh bag system was developed (see Fig. 1a). The bags consisted of 50 μm nylon mesh with an inner compartment (5 × 4 cm) containing homogenised soil from the substrate the bag was embedded in (6 and 10 g for organic and mineral horizon soils respectively) and surrounded by an outer mesh bag (6 × 5 cm) containing 14 g of 1 mm borosilicate beads (Sigma-Aldrich Co.). These beads were washed with 1 M HCl overnight to eliminate any contamination occurring during manufacturing, rinsed with deionised water until the pH was neutral and dried at 100°C for 48 h. The two mesh bags were

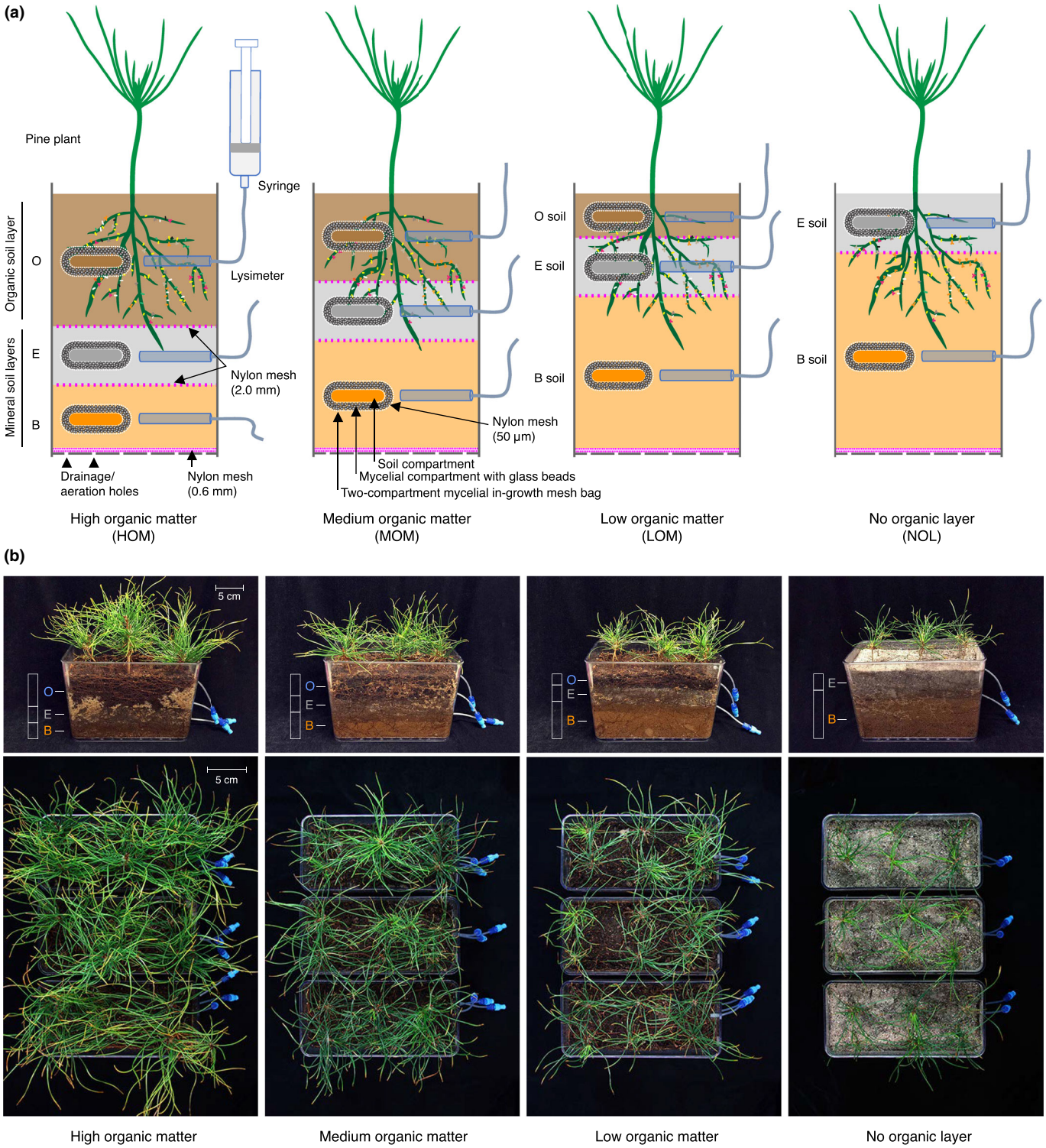

Fig. 1 Schematic representation showing the design of the microcosm system and experimental treatments. (a) *Pinus sylvestris* plants were grown in acrylic containers with a reconstructed boreal podzol profile using organic (O) and mineral (E and B) horizon soils from a boreal forest in Sweden. A gradient of organic matter (OM) availability was created by manipulating the relative amount of O horizon material: HOM, high organic matter; MOM, medium organic matter; LOM, low organic matter; NOL, no organic layer ($n = 3$). Control microcosms without plants were also set up. The O, E and B horizons were separated by 2.0 mm nylon mesh (to facilitate destructive sampling of roots and soils from each horizon at harvest). Lysimeters were inserted in each horizon for soil solution sampling. For harvesting of clean mycelium free of adhering soil particles, two-compartment mycelial in-growth mesh bags were designed – the inner mesh bag contained soil, and the outer 'mycelial compartment' contained glass beads allowing harvesting of clean mycelium. Two mesh bags were embedded in each soil horizon. There were drainage/aeration holes at the base of microcosms and two nylon mesh sheets were placed to prevent loss of soil through the holes. (b) Actual plant growth following 14 months of incubation in phytotron, showing the positive influence of increased amounts of OM.

heat-sealed, and the total weight was recorded. The rationale behind designing the two-compartment mesh bag system was that hyphae/mycelium, after entering the outer mesh bag compartment (containing glass beads), would continue growing towards the central mesh bag (containing soil) to capture nutrients. This approach is expected to result in mycelium with elemental concentrations/composition comparable to mycelium growing in contact with natural soil. Obviously, recovery of clean mycelium from the glass bead-compartment (without contaminating, adhering soil particles) is much easier and harvested mycelium can reliably be used for any downstream chemical/isotopic or molecular analyses.

Microcosms with reconstructed podzol horizons

Freshly sieved soil from the different horizons was transferred into 40 2.1 l (200 × 100 × 142 mm ($L \times W \times H$)) transparent acrylic containers. Two to three 5 mm holes were drilled in the narrow end of each container to allow for soil solution sampling – the number and orientation depending on treatment. Additional holes were drilled in the base for aeration and drainage. Four treatments were designed to create a gradient of OM availability with high, medium and low amounts of OM (HOM, MOM and LOM respectively). No organic layer (NOL) was present in the fourth treatment (see Fig. 1a). This was done by altering the volume of the O horizon. Eight microcosms were constructed per treatment, four containing six *Pinus sylvestris* plants each, and four controls without plants. Before the addition of soil, two nylon mesh sheets (0.5 mm thick, 0.6 mm pore size) were placed at the base of each microcosm to prevent soil loss through drainage holes and to aid harvesting. B horizon soil was then added in variable quantities to keep the overall soil volume constant, 250 g in HOM, 650 g in MOM, 1050 g in LOM and 1450 g in NOL treatments. A nylon mesh sheet (1.0 mm thick, 2.0 mm pore size) was placed on the surface of the B soil maintaining stratification and aiding harvesting (of roots and soil), followed by 800 g E horizon soil regardless of treatment. A second nylon mesh (1.0 mm thick, 2.0 mm pore size) was placed between the E and O horizon soil, which was added in variable quantities depending on treatment (600 g in HOM, 400 g in MOM, 200 g in LOM and 0 g in NOM). The combined total volume of O, E and B horizon soils was the same in every treatment. Two mesh bags and a Rhizon® pore water sampler (Rhizosphere Research Products, the Netherlands) were embedded in each soil layer, facilitating extraction of root/soil-free mycelium and soil solution respectively. Pine seedlings were planted at a standard depth (2–3 cm) either in O horizon (HOM, MOM, LOM treatments) or in E horizon (in the NOL treatment). In Fig. 1(a), the distribution of roots and shoots is schematic, showing that roots were able to grow through the mesh partitions, but does not show differences in growth or distribution related to treatments. Each microcosm was wrapped in aluminium foil and the soil surface was covered with a thick black plastic sheet to prevent exposure of developing mycelia to light and to prevent growth of algae and mosses. The water-holding capacity of each treatment combination of organic and mineral soil was estimated by the construction of four plant-free microcosms before the experiment. Microcosms were incubated in a phytotron for 14 months with a 250 µmol m^{-2} s^{-1} PAR 18 h : 6 h, light : dark cycle and day : night temperature of 18°C : 16°C. Soil moisture was kept constant by gravimetric watering with deionised water. Air moisture was maintained through natural evaporation from randomly placed plastic cups filled with deionised water. The positions of the microcosms were randomised on a weekly basis to reduce the impact of environmental differences within the phytotron.

$^{13}CO_2$ pulse labelling of plants

In the final month of incubation, three replicate microcosms of each treatment were randomly selected for $^{13}CO_2$ pulse labelling, and the remaining microcosms were moved to a separate plant growth room for $\delta^{13}C$ natural abundance measurements. The microcosms were placed in a transparent, airtight acrylic chamber and subjected to $^{13}CO_2$ pulse labelling. The chamber was equipped with fans to promote air circulation, and additional lights to support photosynthesis. Continuous exposure of plants to 99 atom% $^{13}CO_2$ (Cambridge Isotope Laboratories Inc., Andover, MA, USA) occurred in 8 h episodes over the course of 3 d, coinciding with the peak photoperiod. During these 8 h periods, total CO_2 concentration was maintained at an average 480 ppm – measured by an infra-red gas analyser (IRGA; EMG-4; PP Systems, Hitchin, UK). Upon depletion to 300 ppm, additional $^{13}CO_2$ gas was added by manual injection using an airtight syringe. Before the initial pulse of $^{13}CO_2$, plants were allowed to deplete the CO_2 to 200 ppm to promote a higher concentration of $^{13}CO_2$ within the chamber for the duration of the $^{13}CO_2$ exposure. The average rate of $^{13}CO_2$ assimilation by plants was 124 ml h^{-1}, determined by IRGA. Following the 3-d course of $^{13}CO_2$ pulse exposure, microcosms were incubated in a phytotron under normal conditions for a further week – a chase period – allowing assimilated ^{13}C to migrate through the plant to microbial associates in the soil in the form of photoassimilates. After this chase period, microcosms were harvested.

Harvesting of microcosms

Microcosms were harvested destructively. Details on sampling of plant, soil and mycelial compartments, and processing of materials for different analyses are provided in Methods S1. Soil solutions were extracted by centrifugation using modified 60-ml syringe barrels that had been acid washed. Soil samples were centrifuged at 10 000 ***g*** for 1 h at 4°C, and the extracted solutions were filtered with 0.45 µm sterile syringe filters before storing at −20°C. Rhizon® pore water samplers were also used for *in situ* sampling of solutions, but for the final destructive sampling, we used centrifugation. This decision was based on the rationale that ectomycorrhizal hyphae can grow into micropores of mineral particles and microsites of soil aggregates – these sites are generally inaccessible to roots – and are assumed to create hotspots of biogeochemical activity due to allocation of plant host derived C.

Chemical analysis of plants, soils, soil solutions and mycelium

Milled solid samples were digested in concentrated HNO_3, and concentrations of Ca, K, Mg, P, Mn and Sr were determined by inductively coupled plasma mass spectroscopy (ICP-AES). Soil solution pH was also measured.

Stable isotope analysis of ^{13}C, ^{15}N and ^{26}Mg

^{13}C isotope enrichment (or natural abundance), ^{15}N natural abundance, and C and N concentrations were measured in samples of shoots and roots (1.0 and 2.0 mg respectively), organic and mineral soils (1.0 and 6.0 mg respectively) following encapsulation of the materials in tin capsules (Elemental Microanalysis, Devon, UK). Soil solution samples from organic and mineral soils (100 and 500 µl respectively) were dried in tin capsules at 80°C for 2 d. Measurements were performed using an elemental analyzer (EuroEA3024; Eurovector, Milan, Italy) connected to a continuous flow Isoprime isotope ratio mass spectrometer (GV-Instruments, Manchester, UK).

Soil solutions were used for Mg isotope measurements. In brief, aliquots of soil solutions were analysed for pH and major cations (Ca, Mg, K and Na) by ICP-AES, and the remaining solution was evaporated to dryness. Residues were dissolved with 3 ml of concentrated HNO_3 and stored at 4°C until Mg isotope purification. Purified Mg (25–50 µg) samples from soil solution were obtained by ion chromatography using a combination of AGMP1-X8 anion-exchange resin (to eliminate trace elements Fe, Cu, Zn, etc.) with 7 M HCl and AG50W-X12 cation exchange resin (to eliminate major cations) with 1 M HNO_3 (Bolou-Bi *et al.*, 2016). The purified Mg solutions were evaporated to dryness and dried samples were diluted with 0.05 N HNO_3 at 200 ppb before analysis using multicollector-inductively coupled plasma mass spectroscopy (MC-ICP MS). Magnesium isotope ratios were measured using the standard-sample bracketing technique with DSM3 standard solution to correct for the instrument mass bias (Galy *et al.*, 2003).

DNA extraction, PCR amplification and high-throughput sequencing

DNA was co-extracted with RNA from soil samples using RNA PowerSoil Total RNA Isolation Kit and RNA PowerSoil DNA Elution Accessory Kit (MoBio Laboratories, Carlsbad, CA, USA), following the manufacturer's protocol. DNA from mycelium samples was extracted using DNeasy Plant Mini Kit (Qiagen) according to the manufacturer's recommendations. Mycelium was freeze-dried and homogenized by milling in 2 ml tubes, before DNA extraction. DNA concentration was measured by NanoDrop (ND-1000 NanoDrop Technologies, USA) and stored in PCR grade H_2O at −80°C until further processing.

The fungal ITS region was PCR amplified using the primers fITS9 (5′-GAACGCAGCRAAIIGYGA-3′; Ihrmark *et al.*, 2012) and ITS4 (5′-TCCTCCGCTTATTGATATGC-3′; White *et al.*, 1990). The ITS4 primer contained an 8-base barcode sequence unique for each sample. Details on PCR reagents and amplification conditions are described in Methods S1. The triplicate PCR products from each sample were pooled and cleaned with Agencourt AMPure Kit (Beckman Coulter, Beverly, MA, USA) according to the manufacturer's recommendations. DNA concentration was determined in each sample by Qubit dsDNA HS Assay using a Qubit Fluorometer (Invitrogen). All the PCR products from differently barcoded samples were pooled in equal concentrations and purified using the EZNA Cycle Pure Kit (Omega Bio-Tek, Norcross, GA, USA) and then eluted twice with 50 µl EB. The quality of the resulting pool and fragment size distribution were analysed using 50 Agilent DNA 7500 Kit with the Agilent 2100 Bioanalyzer system (Agilent Technologies, Santa Clara, CA, USA). The pooled sample was sequenced at SciLifeLab, NGI-Uppsala, Sweden, and underwent high throughput sequencing, using 3 SMRT cells of PacBio Sequel System (Pacific Biosciences, San Diego, CA, USA) according to the manufacturer's recommendations. The library preparation and adaptor ligation were also carried out at SciLifeLab, NGI-Uppsala, Sweden.

Bioinformatic and fungal functional guild analyses

In total, 1010 556 reads were obtained from PacBio sequencing of DNA from soil and mycelial samples, and after initial quality filtering and removal of chimaeras 516 998 reads remained. After removal of nonfungal sequences and singletons, 263 435 and 235 355 sequences were obtained from soil and mycelial samples respectively for downstream analysis. The sequencing data were analysed using the QIIME pipeline (Caporaso *et al.*, 2010). In brief, the command 'demultiplex_fasta.py' was used to demultiplex sequences based on barcodes and 'adjust_seq_orientation.py' to reverse complement sequences that remained unassigned. After combining both forward and reverse complemented reads in one file, the command 'split_libraries.py' was used to split libraries according to sample barcodes as listed in the mapping file. Chimeric sequences were identified using VSEARCH (Rognes *et al.*, 2016) in MOTHUR (Schloss *et al.*, 2009) and a UCHIME reference dataset (Nilsson *et al.*, 2015). The sequences were clustered into operational taxonomic units (OTUs) by UCLUST (Edgar, 2010) using the command 'pick_otus.py' with the *denovo* option, as implemented in QIIME, using a 97% sequence similarity criterion. The representative sequences of all OTUs were chosen with command 'pick_rep_sets.py' and an OTU table was constructed with command 'make_otu_table.py'. Individual sequences were classified taxonomically using the 'classify.seqs' command in MOTHUR (Schloss *et al.*, 2009; confidence threshold 80) using the UNITE fungal ITS reference database (Kõljalg *et al.*, 2013). Nonfungal OTUs were removed manually from the OTU table, and the singletons were removed in QIIME using command 'filter_otus_from_otu_table.py'. The filtered OTU table was rarefied using command 'single_rarefaction.py' and from this rarefaction curves were generated using command 'multiple_rarefactions.py'. All samples were rarefied to an equal number of sequences (4493) before further analysis. Taxa summary tables for downstream analyses of sequences were generated using 'summarize_taxa.py', and taxa plots were generated using 'summarize_taxa_through_plots.py'. For

functional guild-based annotation of the OTUs, all OTUs were parsed using FUNGuild tools (Nguyen *et al.*, 2016). The resulting data set contained the following dominant functional guilds: ectomycorrhizal, saprotroph, ericoid mycorrhizal, pathogen and some fungi were assigned to multiple guilds (e.g. ectomycorrhizal-ericoid mycorrhizal, ectomycorrhizal-saprotroph and pathogen-saprotroph). Fungi that could not be classified to any known guild (due to lack of sufficient ecological and/or taxonomic characterisation) were grouped as 'unassigned' and less abundant guilds were grouped as 'others'. All annotations were checked manually against published information on taxonomy, ecology and habitat of different fungal species.

Data analysis and statistics

Effects due to treatments on each parameter were evaluated by analysis of variance (ANOVA), linear regression analysis was used to assess relationship between pairs of selected parameters, and principal component analysis (PCA) was used to assess correlation among several parameters (Jmp Pro 15 statistical package). Using rarefied abundance data, beta diversity patterns were analysed by nonmetric multidimensional scaling (NMDS) ordinations with Bray–Curtis dissimilarity measure. The differences in fungal community composition in O, E and B horizon soils (or mycelial samples from each horizon) within a reconstructed podzol microcosm or in a particular horizon soil across the treatments were estimated using nonparametric analysis of similarity (ANOSIM) and permutational multivariate analysis of variance (PERMANOVA) with 9999 permutations (Past v.4.03 statistical package). The fungal taxa that differed significantly ($P < 0.05$) in relative abundance across the treatments were identified using the command 'group_significance.py' with ANOVA implementation in Qiime (Caporaso *et al.*, 2010).

Results

Increasing availability of OM significantly increased root, shoot and mycelial biomass (Figs 1b, 2a,b), with the largest and statistically strongest effect on mycelial biomass occurring in the mineral B horizon (Fig. 2b,c). There was a 121% increase in mycelial biomass in the treatment with high amounts of OM (HOM) compared with the treatment containing medium amounts of OM (MOM) and 45% of the total mycelial biomass was found in the B horizon. This total increase occurred although the volume of B horizon soil was only 38% of that in the MOM treatment, resulting in a mycelial density in the B horizon ($mg\,cm^{-3}$) that was 3.64 times higher in the HOM treatment than in the MOM treatment (Fig. S1a). Plant N content increased significantly in response to increased amounts of OM (Fig. 2d), suggesting that improved supply of N was driving plant growth. Apart from the fact that the O horizon contained 16 times as much N as the E and B horizons (Table S1), additional support for the idea that the O horizon was the source of the mobilised N is provided by differences in stable isotope signatures. Plants in HOM systems had more depleted $\delta^{15}N$ signatures, which were more like those of soil from the O horizons than those of the mineral horizons (Fig. S1b–d). Interestingly, the plant N use efficiency (shoot biomass production per unit N taken up) was positively related to the mycelial biomass (Fig. 2e), suggesting that plants with access to greater amounts of OM, in addition to more N, also had increased access to other growth-limiting nutrients (essentially base cations and P).

Pulse labelling of ectomycorrhizal *Pinus sylvestris* plants with $^{13}CO_2$ allowed us to monitor the effects of different OM availability on the allocation of recently photosynthetically derived C to plant roots, soil (mycelial biomass) and soil solution (Fig. 3). Increased amounts of ^{13}C were assimilated by the shoots of larger plants (Fig. 3a) and ^{13}C allocation to the soil and soil solution in the B horizon was significantly higher in the HOM systems (Fig. 3b,c). ^{13}C allocation was positively related to the higher mycelial biomass in the B horizon, but not in the O and E horizons (Fig. 3d,e). Moreover, a PCA showed that N use efficiency was strongly correlated with the amount of ^{13}C allocated to O and B horizon soil and soil solutions, with the patterns mainly driven by the HOM systems (Fig. 3f,g).

Correlations between plant base cation content (Fig. 4a) and P content (Fig. 4b) and mycelial biomass were highly significant for the B horizon, significant for the E horizon but not statistically significant for the O horizon. Similar relationships were obtained for the individual base cations Ca, K and Mg (Fig. S2), suggesting that the increased mycelial biomass produced in the mineral horizons, especially the B horizon, played a functional role in mobilising base cations and P that were supplied to the plants. The strong association of plant acquisition of Ca, K, Mg and P with both the mycelial biomass in, and ^{13}C allocation to, the B horizon (as depicted in the PCA; Fig. 4c,d) indicates the importance of C allocation to fungal mycelium for mineral weathering in deeper soil.

Further evidence that mobilisation in the B horizon contributes to improved acquisition of base cations, and Mg in particular, is provided by analyses of $\delta^{26}Mg$ (‰) signatures in the soil solution (Fig. 5). Ectomycorrhizal fungi have been reported to discriminate against heavier isotopes of Mg, such as ^{26}Mg, during Mg^{2+} uptake (Fahad *et al.*, 2016). Accumulation of ^{26}Mg in soil solution (increased $\delta^{26}Mg$ signature) is therefore a sign of active uptake of Mg^{2+}. In the B horizon, we found a significant positive relationship between soil solution $\delta^{26}Mg$ signature and plant/root biomass, plant Mg content and total ^{13}C in soil and soil solution (mycelial biomass was marginally non-significant), but no significant relationships in the O and E horizons (Fig. 5a–e). The higher amounts of ^{13}C and larger amounts of mycelium in the B horizon of HOM systems, coupled with the enrichment of ^{26}Mg in the B horizon soil solution, suggest that plants with access to greater amounts of OM could allocate more C to enhance mobilisation and uptake of Mg in the B horizon. Clear negative relationships between the $\delta^{26}Mg$ signature in soil solution and contents of Ca, Mg, Mn and Sr (Fig. S3a–f) indicated that accumulation of ^{26}Mg in solution was related to higher uptake of not only Mg, but also other elements. In systems without plants (Fig. S3g–l), there were no treatment effects in the B horizon, but some evidence

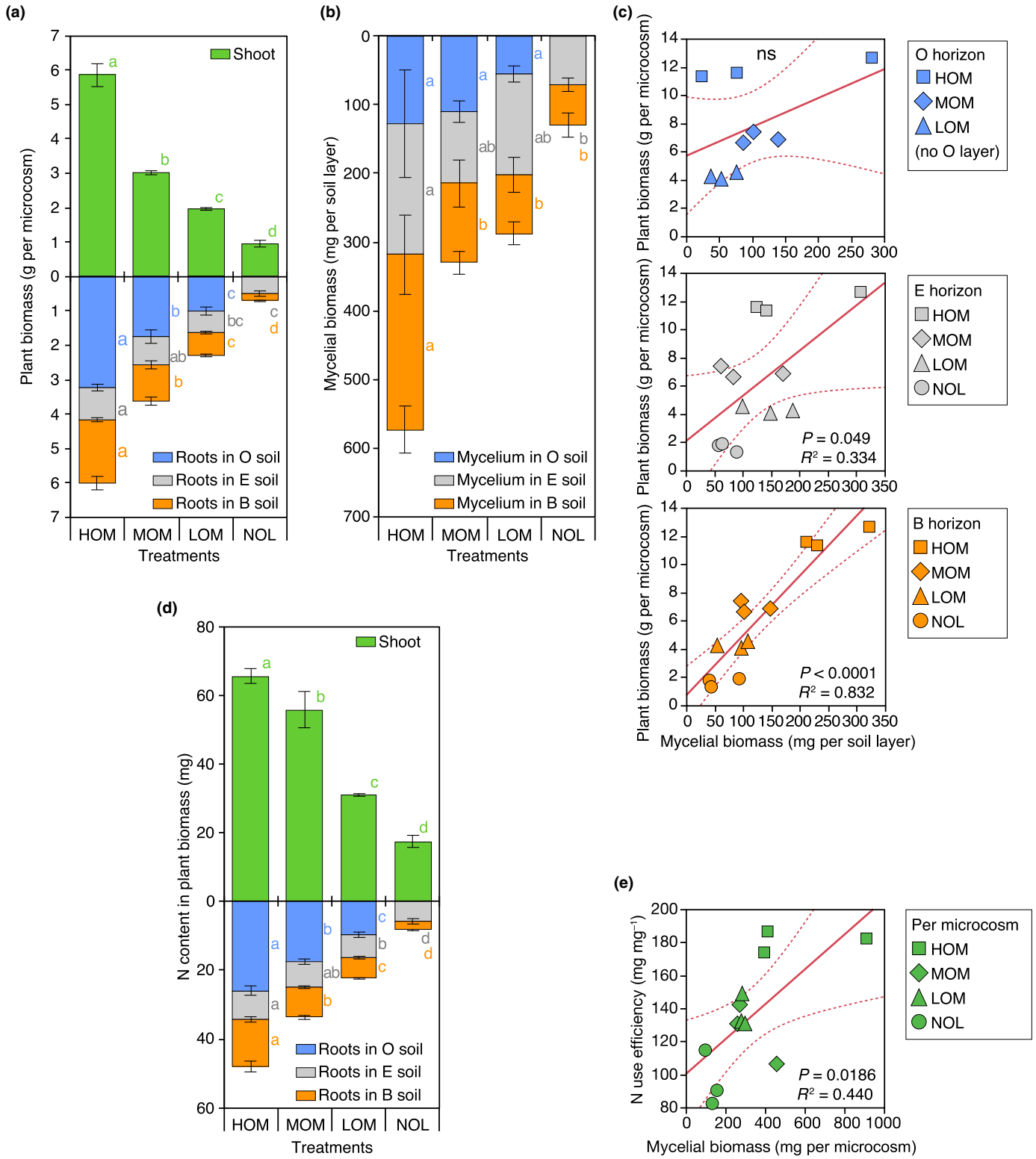

Fig. 2 Effects of organic matter (OM) availability on *Pinus sylvestris* growth and mycelial biomass distribution in podzol profiles. Root, shoot and mycelial biomass (a, b) increase significantly with increasing availability of OM, with the statistically strongest effect occurring in the mineral B horizon (c). Similar significant increases in plant nitrogen (N) content occur in response to increased amounts of OM (d). Nitrogen use efficiency (production of plant biomass per unit N taken up) is improved in plants with adequate access to OM since improved mycelial growth in mineral soil horizons enables access to additional resources (e) in the form of base cations and phosphorus. A gradient of OM availability was created by manipulating the relative amount of O horizon material: HOM, high organic matter; MOM, medium organic matter; LOM, low organic matter; NOL, no organic layer ($n = 3$). Error bars are ±SE and different letters denote differences among means ($P < 0.05$; ANOVA). Dotted lines (c, e) indicate 95% confidence intervals; ns indicates not significant.

New Phytologist

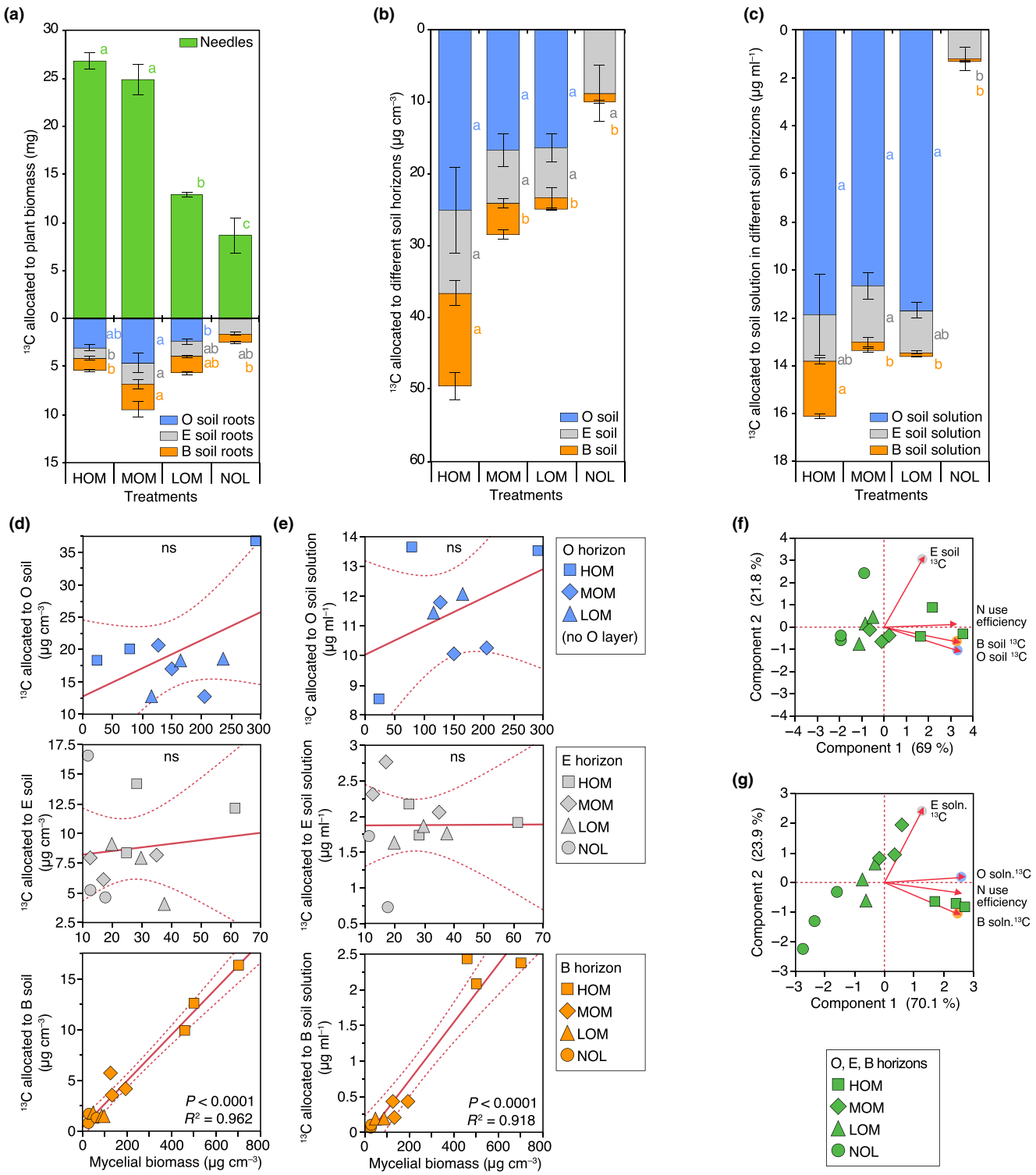

Fig. 3 Allocation of photosynthetically derived carbon to different plant and soil compartments and its relationship with mycelial biomass and nitrogen use efficiency. Ectomycorrhizal *Pinus sylvestris* plants (growing in podzol profiles with varying amounts of O horizon organic matter (OM)) were pulse labelled with $^{13}CO_2$. (a) Allocation of ^{13}C to plant shoots and roots in different soil horizons. (b) Allocation of ^{13}C to organic and mineral soil horizons colonised by mycelium. (c) Allocation of ^{13}C to soil solution in each soil horizon (containing ^{13}C-labelled mycelial and root exudates). (d, e) Linear regression relationships between ^{13}C allocated to soil and soil solution in each soil horizon and mycelial biomass (per cm^3), respectively. (f, g) Principal component analyses illustrate the association of treatment effects with variation in nitrogen use efficiency and ^{13}C content in soil (f) and soil solution (g) in organic and mineral soil horizons. A gradient of OM availability was created by manipulating the relative amount of O horizon material: HOM, high organic matter; MOM, medium organic matter; LOM, low organic matter; NOL, no organic layer ($n = 3$). Histograms (a–c) show mean values (error bars are ±SE), and different letters denote significant treatment differences within compartments ($P < 0.05$; ANOVA). Dotted lines (d, e) indicate 95% confidence intervals; ns indicates not significant.

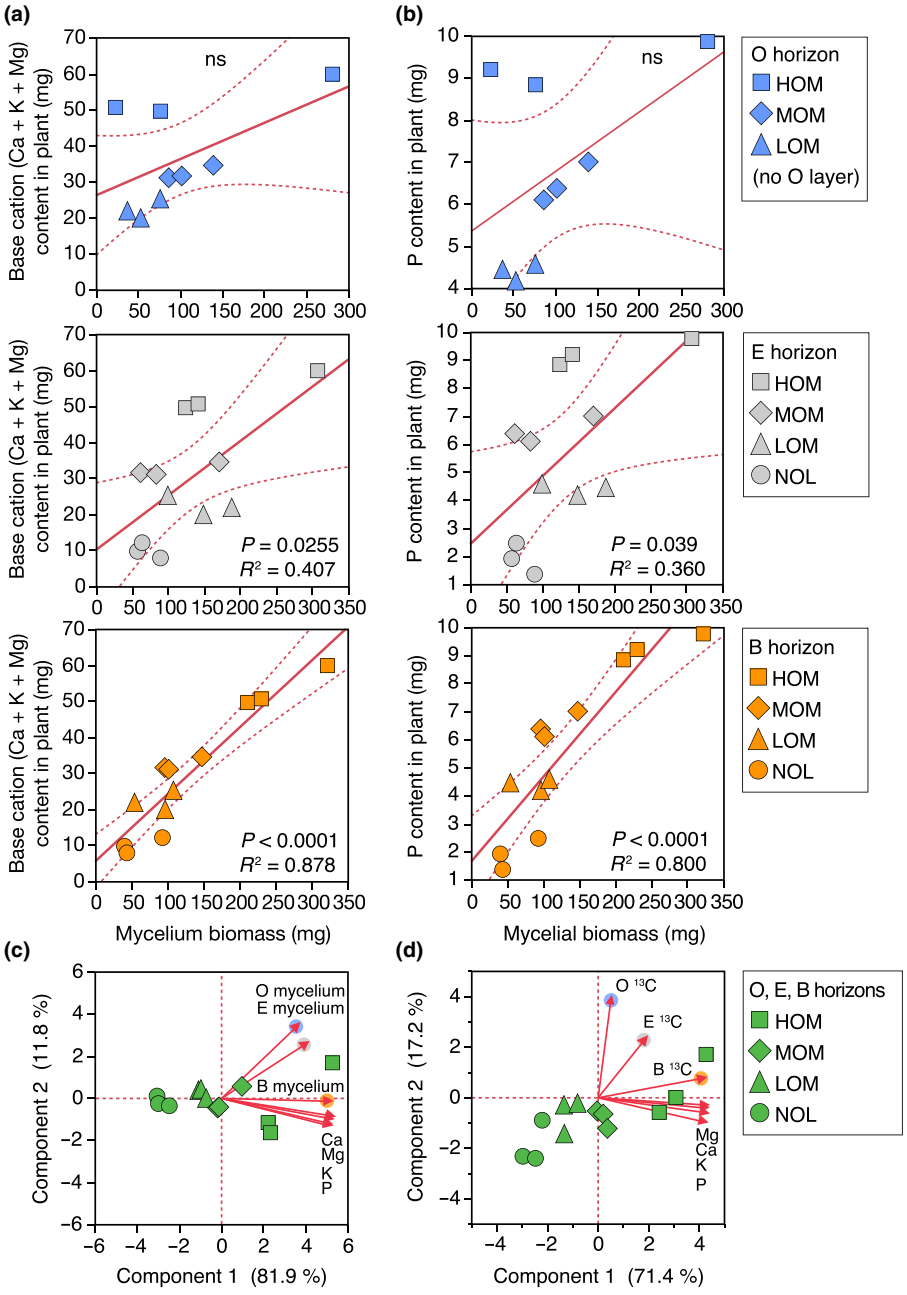

Fig. 4 Positive effects of increasing organic matter (OM) availability on mycelial biomass, carbon allocation and acquisition of base cations and phosphorus by ectomycorrhizal *Pinus sylvestris* plants growing in podzol profiles with varying amounts of O horizon OM. Acquisition of base cations (Ca + K + Mg) (a) and phosphorus (b). Dotted lines (a, b) indicate 95% confidence intervals; ns indicates not significant. Effects are highly significant in the mineral B horizon, less significant in the mineral E horizon but not statistically significant in the O horizon. Principal component analyses show highly significant treatment variation in mycelial biomass (c) and ^{13}C in soil plus soil solution (d) in the B horizon, associated with changes in plant content of Ca, Mg, K and P. A gradient of OM availability was created by manipulating the relative amount of O horizon material: HOM, high organic matter; MOM, medium organic matter; LOM, low organic matter; NOL, no organic layer ($n = 3$).

of nutrient mobilisation by saprotrophic fungi in the O horizon that was proportional to the amount of OM. Elemental analysis of soil samples (Table S1) suggests that significant pools of base cations (in particular Ca) and P exist in the O horizon. However, the $\delta^{26}Mg$ signatures in soil solution (Figs 5, S3a–f) and the proportional distribution of the solubilised elements (Table S2), suggest that it is the elements efficiently removed from the solution in the B horizon, not the O horizon, that accumulated in the plant biomass.

Overall, 704 fungal taxa were distinguished. Nonmetric multidimensional scaling ordinations of fungal community composition in the O, E and B horizons (Figs 6, S4a) illustrate strongly significant statistical differences between soil horizons, as well as significant treatment effects in both the O and B horizons. The changed community composition in the B horizon was particularly strongly associated with variation in plant contents of Ca, Mg, K, N and P, as indicated by the lengths of the vectors (Fig. 6a). Linear regression analyses showed a significant positive relation between total plant biomass and the relative abundance of the ectomycorrhizal guild (Fig. 6b) in the B horizon, while the saprotrophic guild in the same horizon (Fig. 6c) showed a negative relation with plant biomass. The occurrence of fungal guilds in other horizons showed no relation to plant biomass. The contrasting relationships of plant biomass with the relative abundance of ectomycorrhizal and saprotrophic fungi in the B horizon are most likely explained by competition between the

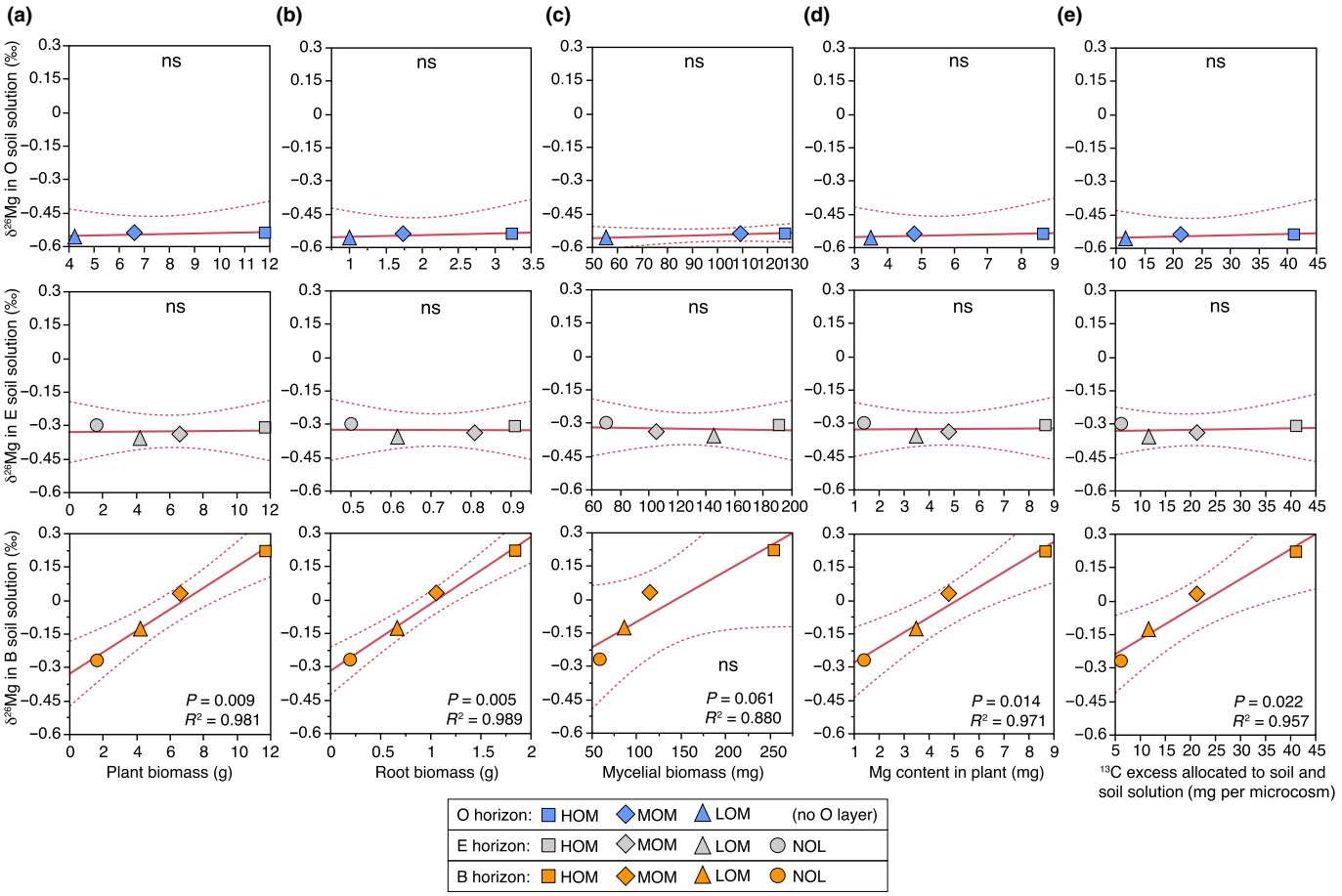

Fig. 5 Increase in δ^{26}Mg isotopic ratio of B horizon soil solution with increasing organic matter (OM) availability. Linear regression relationships between the δ^{26}Mg signature of pooled soil solution samples ($n = 3$) from organic (O) and mineral (E and B) horizons and plant biomass (a), root biomass (b), mycelial biomass (c), Mg content in plant biomass (d) and ^{13}C content in soil and soil solution (e) demonstrate statistically significant positive relationships for all parameters in the B horizon, except mycelial biomass, which was marginally nonsignificant ($P < 0.061$). The data suggest that the positive effects of increasing OM availability on the parameters caused increased plant growth, carbon allocation and mineral weathering, leading to increased Mg uptake. The relationships are not significant in the O and E horizons. Ectomycorrhizal *Pinus sylvestris* plants were grown in podzol profiles with a gradient of OM availability that was created by manipulating the relative amount of O horizon material: HOM, high organic matter; MOM, medium organic matter; LOM, low organic matter; NOL, no organic layer. Dotted lines indicate 95% confidence intervals; ns indicates not significant.

two guilds, since available C in OM is low in the B horizon, but ectomycorrhizal fungi can receive C allocated from their plant hosts. The high relative abundance of ectomycorrhizal fungi in the B horizon, particularly in the HOM treatment where C allocation is increased, suggests that the base cation and P mobilisation is driven primarily by ectomycorrhizal fungi. The 25 most abundant taxa in soil accounted for *c.* 90% of all sequences, and the impact of OM reduction in the O horizon was strongest on relative abundance of these taxa in the mineral soil, in which 14 and 7 taxa were significantly impacted in the B and E horizons respectively, and only three taxa were significantly influenced in the O horizon (Fig. S5). This suggests that fungi in deeper mineral soil are more sensitive to changes in OM than taxa in the top organic horizon. The ectomycorrhizal species *Piloderma sphaerosporum* was the most abundant species in the O horizon, while *Suillus bovinus* was the most abundant in the E and B horizons (Fig. S5). Two-compartment mesh in-growth bags were inserted into each soil horizon for mycelial biomass determination. These were intensively colonised by 441 fungal taxa in total, dominated by *P. sphaerosporum* and *S. bovinus*, with the ectomycorrhizal fungal guild accounting for over 80% of the analysed amplicons (Fig. S6). Total plant contents of Ca, K, Mg and P were positively correlated with the proportional abundance of ectomycorrhizal amplicons in the B horizon (Fig. S7). The proportional abundance of ectomycorrhizal amplicons in the B horizon was also negatively correlated with the soil solution pH (Fig. S8).

Discussion

Human appropriation of net primary production is increasingly being driven by changes in land use intensity rather than changes in land use area (Kastner *et al.*, 2021) and intensification of forestry is no exception to this trend. Soil OM is generally assumed to be important to forest productivity, but its direct influence has been difficult to demonstrate because it is both a cause and effect

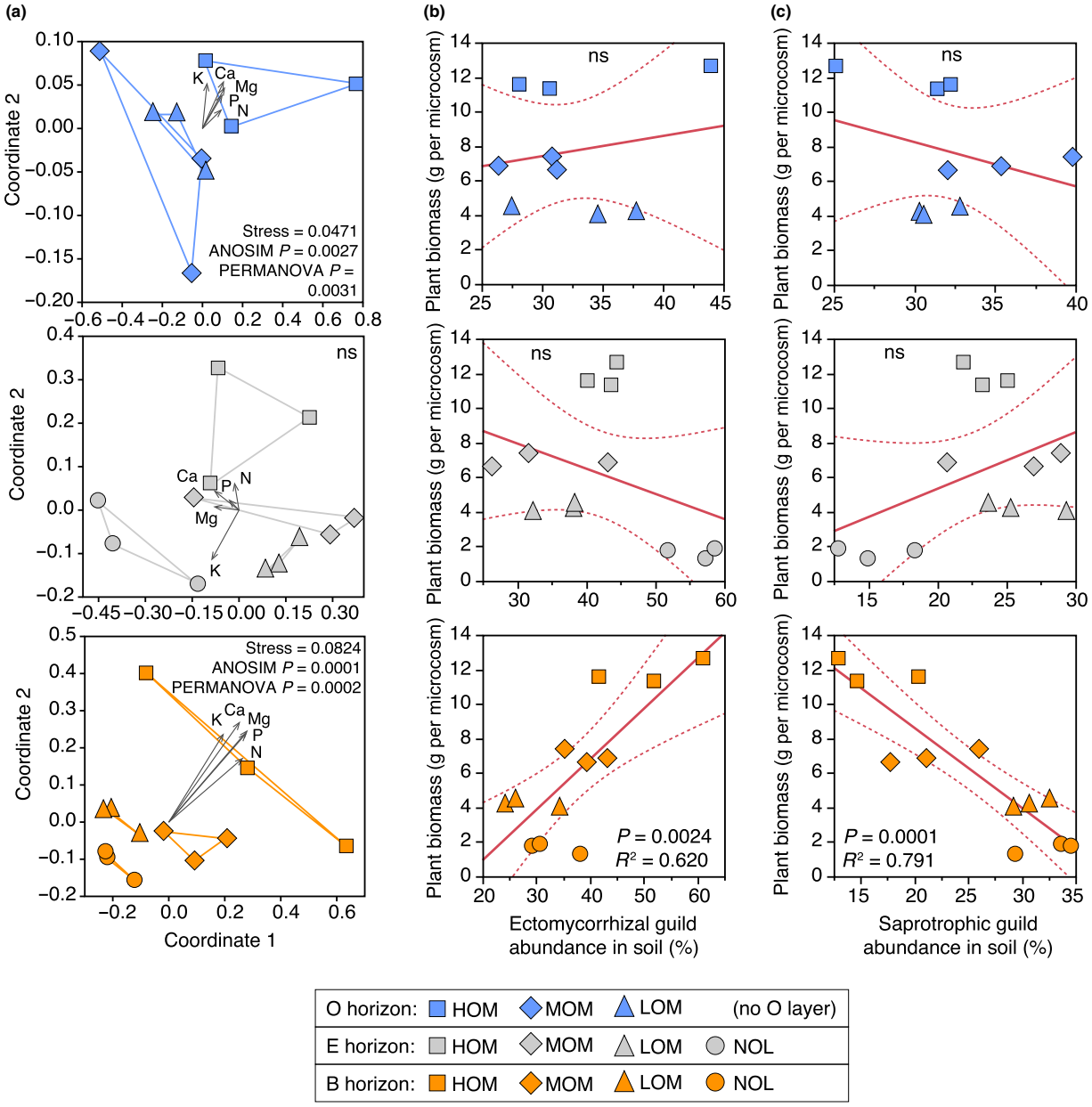

Fig. 6 Influence of changed availability of organic matter (OM) on soil fungal community composition and relative abundance of different functional guilds. (a) Nonmetric multidimensional scaling ordinations of fungal community composition in the organic (O), and mineral (E and B) horizons of podzol profiles in relation to changes in OM availability from high organic matter (HOM) to medium organic matter (MOM) to low organic matter (LOM) to no organic layer (NOL) ($n = 3$). Significant treatment differences ($P < 0.05$) occur in the O and B horizons, and the arrow lengths indicate the strength of the contribution of different elements to the overall treatment differences (strongest in the B horizon). (b, c) Linear regression relationships between total plant biomass and the relative abundance of the ectomycorrhizal and saprotrophic fungal guilds, respectively. There is a highly significant positive relationship for the ectomycorrhizal guild and a highly significant negative relationship for saprotrophs in the B horizon, but no significant relationships in other horizons. Dotted lines indicate 95% confidence intervals; ns indicates not significant.

of productivity and the relationship is complex and site-specific (Grigal & Vance, 2000). The present study provides novel evidence, based on fractionation of stable isotopes, of ectomycorrhizal weathering and uptake of naturally occurring base cations from mineral forest soil by indigenous fungal communities. This weathering is driven by sinks generated by ectomycorrhizal mobilisation of N from the organic horizon, and our experiments show clearly how changes in OM availability in the O horizon influence fungal C allocation to deeper mineral horizons, as well as the abundance of different functional fungal guilds. Ectomycorrhizal fungi play an important role in mobilising N from organic substrates and our results support the well-established idea that photosynthetically derived C transferred to the ectomycorrhizal fungal symbionts drives this process (Bending & Read, 1995; Rineau *et al.*, 2013; Shah *et al.*, 2016; Nicolás *et al.*, 2018).

Selective allocation of photosynthetically derived C through ectomycorrhizal fungal networks to patches of added minerals has been shown in experimental microcosms inoculated with single fungal species (Rosling *et al.*, 2004; Smits *et al.*, 2012) and shown to increase the weathering of apatite and subsequent uptake of P by plants (Smits *et al.*, 2012). However, there are few mechanistic studies of mycorrhizal weathering in natural soils. Uptake and transport of Mg through fungal hyphae to *Picea abies* seedlings inoculated with the mycorrhizal fungus *Paxillus involutus* have been shown in sand-filled microcosms supplied with ^{25}Mg-labelled nutrient solution (Jentschke *et al.*, 2000), but the present experiment demonstrates the capacity of indigenous fungal communities to mobilise naturally occurring Mg from mineral soil and transport it to tree seedlings. The higher relative proportion of base cations and P remaining in the O horizon solution (Table S2) are consistent with previous studies in which accumulation of organic P has been reported in O horizon/humus layer of boreal forests (Giesler *et al.*, 2002, 2004; Vincent *et al.*, 2022), and different geochemical explanations have been proposed. Both Al and Fe appear to have a stabilising effect that protects organic P from microbial degradation (Vincent *et al.*, 2012), and this could be one effect slowing mycelial uptake from this horizon. We speculate that even though the base cations and P are in a dissolved state in the O horizon solution, they may be bound in relatively recalcitrant organic complexes requiring more intensive enzymatic degradation of dissolved OM. High competition with saprotrophs in the O horizon may also restrict successful competition for, and removal of P from soil solution by ectomycorrhizal fungi. In the present study, the soil solution pH was negatively correlated with the proportional abundance of ectomycorrhizal amplicons in the B horizon to the (Fig. S8) suggesting that the mobilisation and uptake of base cations and P may have been associated with acidification due to secretion of organic acids by the predominantly ectomycorrhizal fungi colonising that horizon (Van Hees *et al.*, 2005). This result is also consistent with pure culture studies demonstrating the superior ability of ectomycorrhizal fungi, compared with saprotrophic species, to mobilise Mg from granite particles (Fahad *et al.*, 2016). The improved access to base cations and P, enabled by the increased mycelial colonisation of the B horizon soil may explain the improved N use efficiency of plants in treatments with greater OM availability.

The way in which C allocation through ectomycorrhizal mycelial networks integrates N mobilisation in the uppermost O horizon and mineral weathering in the deeper B horizon is summarised in Fig. 7. Our results demonstrate that weathering of base cations in the B horizon can be upregulated in response to demand induced by improved N supply from the O horizon. In both processes, C allocation from the host plant to mycorrhizal fungi plays an essential role. Conversely, it is apparent that, where

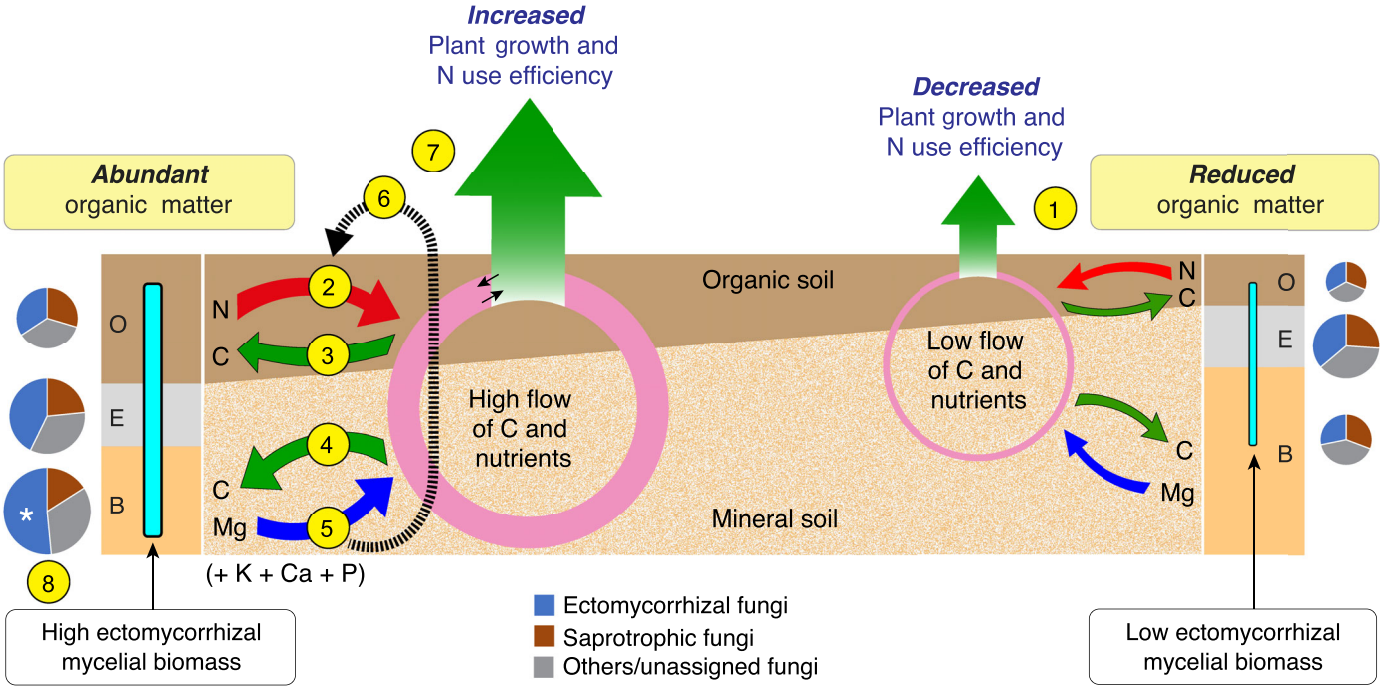

Fig. 7 Conceptual illustration of the integrating role of ectomycorrhizal fungi in organic N mobilisation and mineral weathering in boreal forest soil. Depletion of organic matter (OM) reduces N supply, leading to reduced plant growth and lower C allocation to ectomycorrhizal fungi, restricting their ability to mobilise base cations from the mineral soil (1). Increased availability of OM improves N supply (2), increasing plant growth and C allocation to ectomycorrhizal fungi (3, 4), enabling them to mobilise increased amounts of Mg from the B horizon soil (5). The increased supply of Mg (and other base cations and P) improves the N use efficiency of the plants (6) – demonstrating how ectomycorrhizal fungi integrate N mobilisation and weathering across soil horizons to improve plant growth (7). The pie charts (8) indicate the proportional abundance of fungal amplicons in different categories and their diameter is proportional to total fungal biomass, demonstrating that, when there is abundant OM, the increased mycelial biomass in the B horizon is primarily due to the ectomycorrhizal guild (indicated by the asterisk).

N supply is limited by low availability of OM, supply of base cations may be more limited by reduced weathering of minerals from deeper horizons rather than by the reduced stocks of base cation containing organic residues *per se*. Measured amounts of Mg in litterfall are small in relation to tree uptake (Helmisaari, 1995) and suggest that the mineral soil weathering potential demonstrated in the present study is crucial for Mg availability. This is underlined by the rapid uptake of Mg from soil solution in the B horizon (Table S2).

Terrestrial weathering of silicates, leading to production of marine carbonates, is thought to have driven long-term sequestration of C, leading to drawdown of global CO_2 levels (Berner, 1997) and enhanced rock weathering (ERW) has been suggested as a possible method to increase sequestration of atmospheric C as part of an integrated strategy to mitigate climate change through CO_2 reduction (Taylor *et al.*, 2016; Beerling *et al.*, 2018, 2020). Our results suggest that enhanced weathering will require adequate N supply from organic substrates, or some other source that does not reduce belowground C allocation, since N fertilization with inorganic fertilisers can reduce the belowground flux of C to soil biota, including ectomycorrhizal fungi (Högberg *et al.*, 2010). Repeated harvesting of organic residues from forests as biofuel may reduce the density of mycorrhizal roots (Mahmood *et al.*, 1999) and the results of the present study suggest that colonisation of deeper mineral soils may also be disrupted, with concomitant effects on base cation supply. Such negative effects may be counteracted by site preparation methods that increase the amount of OM around the roots and have been shown to have long-term (30 yr) positive effects on plant survival and tree production (Hjelm *et al.*, 2019).

Ectomycorrhizal fungi have been postulated to play an important part in weathering, and even in pedogenesis (Leake & Read, 2017), but there are few detailed studies of mycorrhizal weathering using natural soils. Microcosm studies with added minerals and microscopic investigation of mineral surfaces suggest that ectomycorrhizal fungi can modify mineral surfaces (Quirk *et al.*, 2012) and that allocation of C to the fungal mycelium colonising in-growth cores filled with basalt is related to the rate of calcium silicate dissolution from the basalt (Quirk *et al.*, 2014). The fungi in the latter experiment were not identified but enhanced weathering of added apatite patches and uptake of mobilised P have been shown in microcosms using *P. sylvestris* seedlings inoculated with the ectomycorrhizal fungus *Paxillus involutus* and growing under axenic conditions (Smits *et al.*, 2012). In our study, we found that high availability of N from OM increased plant C allocation to mycorrhizal mycelial biomass in deeper mineral horizons, resulting in increased mobilisation of Mg, Ca, K and P, and we identified the fungal communities involved, but we did not quantify long-term C sequestration. The ectomycorrhizal taxa *P. sphaerosporum and S. bovinus* that were dominant in organic and mineral horizons respectively, are common in boreal forest soils (Marupakula *et al.*, 2017, 2021). Some *Suillus* spp. have been found to play a role in weathering of apatite, biotite or granite (Wallander *et al.*, 2003; Balogh-Brunstad *et al.*, 2008; Fahad *et al.*, 2016) while *Piloderma* spp. have been reported to produce extracellular proteases and can improve the ability of *Pinus sylvestris* to utilise N from organic sources such as proteins (Heinonsalo *et al.*, 2015) and can also mobilise base cations and P from granite (Fahad *et al.*, 2016). However, many of these studies are based on pure culture systems, and generalisations about the functional role of individual species should be made with caution, since a high degree of phenotypic plasticity can be exhibited under different environmental conditions.

The climate mitigation effects of enhanced weathering of silicates are likely to be influenced by different biological processes (Vicca *et al.*, 2022). Symbiotic N fixation has been demonstrated to drive mobilisation of rock-derived nutrients (Perakis & Pett-Ridge, 2019), and it is likely that the effect we demonstrate here involving N mobilisation by ectomycorrhizal fungi will be even bigger since the mobilisation of N from organic substrates by ectomycorrhizal fungi is a fundamental and well-documented process driving tree growth (Lindahl & Tunlid, 2015). Interestingly, the short-term changes in availability of OM in our study appear to have the same effect as the long-term changes, including the evolution of larger, better developed mycelial systems and build-up of OM, that have been postulated to drive the development of biological weathering over evolutionary time (Leake & Read, 2017; Finlay *et al.*, 2020). Belowground C allocation to the rhizosphere leads to formation of stable soil C more efficiently than aboveground inputs of C (Sokol & Bradford, 2019), and associations between microbially derived OM and minerals form a large pool of slowly cycling C (See *et al.*, 2022). See *et al.* (2022) argue that there is a need for more spatially explicit information on environmental drivers of fungal mycelial exploration since fungi have a strong influence on the amounts and type of C deposited on minerals. The present study demonstrates increased mycelial C allocation to deeper mineral soil, and interactions between plant-derived C compounds and mineral soil leading to mobilisation of base cations, but further studies are required to examine the precise mechanisms involved, and the long-term stability of C ultimately associated with the minerals. Although weathering of minerals, not stabilisation of OM, was the primary focus of the present study, our results do provide new, spatially explicit information on the distribution, species composition and patterns of C distribution in ectomycorrhizal fungal mycelia colonising boreal forest soils, as well as new information on factors that drive C allocation, mycelial growth, fungal mobilisation- and plant uptake of mineral nutrients.

Acknowledgements

Funding was provided by The Swedish Research Council for Environment, Agricultural Sciences and Spatial Planning (FORMAS) grant nos. 2011-01691 (KB, RDF) and 2014-1272 (RDF, SM) and the Swedish University of Agricultural Sciences (SLU). The authors would like to acknowledge the support of the National Genomics Infrastructure (NGI)/Uppsala Genome Center and UPPMAX for providing assistance in massive parallel sequencing and computational infrastructure. Work performed at NGI/Uppsala Genome Center has been funded by RFI/VR and Science for Life Laboratory, Sweden. This article is dedicated

to the life, work and memory of Prof. Torgny Unestam (1931–2023), friend, mentor and colleague at SLU.

Competing interests

None declared.

Author contributions

SM and RDF conceived the original idea. SM designed and constructed the microcosms. ZF and SM performed the experiment. ZF processed samples for chemical/isotopic analyses and collected the data. SM and ZF performed the statistical analyses with input from RDF. SM performed the molecular and bioinformatic analyses, with input from KK. EBB-B performed the ^{26}Mg analyses, with input from SJK and KB. AE performed the ^{13}C and ^{15}N analyses. SM and RDF supervised ZF and KK. SM, AE and RDF drafted the manuscript with input from all other authors.

ORCID

Kevin Bishop https://orcid.org/0000-0002-8057-1051
Emile B. Bolou-Bi https://orcid.org/0000-0001-7803-3214
Alf Ekblad https://orcid.org/0000-0003-4384-5014
Zaenab Fahad https://orcid.org/0009-0000-5835-5160
Roger D. Finlay https://orcid.org/0000-0002-3652-2930
Stephan J. Köhler https://orcid.org/0000-0001-9707-9023
Katharine King https://orcid.org/0009-0009-8075-9466
Shahid Mahmood https://orcid.org/0000-0001-6280-4387

Data availability

The PacBio sequencing data files have been submitted to the European Nucleotide Archive (ENA) at EMBL-EBI (www.ebi.ac.uk) and are available under the study accession no. PRJEB59040. Experimental data of this study are available via figshare (doi: 10.6084/m9.figshare.22012829).

References

Achat DL, Martel S, Picart D, Moisy C, Augusto L, Bakker MR, Loustau D. 2018. Modelling the nutrient cost of biomass harvesting under different silvicultural and climate scenarios in production forests. *Forest Ecology and Management* **429**: 642–653.

Akselsson C, Belyazid S, Stendahl J, Finlay RD, Olsson B, Erlandsson Lampa M, Wallander H, Gustafsson J-P, Bishop K. 2019. Weathering rates in Swedish forest soils. *Biogeosciences* **16**: 4429–4450.

Averill C, Turner BL, Finzi AC. 2014. Mycorrhiza-mediated competition between plants and decomposers drives soil carbon storage. *Nature* **505**: 543–545.

Balogh-Brunstad Z, Keller CK, Dickinson JT, Stevens F, Li CY, Bormann BT. 2008. Biotite weathering and nutrient uptake by ectomycorrhizal fungus, *Suillus tomentosus*, in liquid-culture experiments. *Geochimica et Cosmochimica Acta* **72**: 2601–2618.

Bastin JF, Finegold Y, Garcia C, Mollicone D, Rezende M, Routh D, Zohner CM, Crowther TW. 2019. The global tree restoration potential. *Science* **365**: 76–79.

Beerling DJ, Kantzas EP, Lomas MR, Wade P, Eufrasio RM, Renforth P, Sarkar B, Andrews MG, James RH, Pearce CR *et al.* 2020. Potential for large-scale CO_2 removal via enhanced rock weathering with croplands. *Nature* **583**: 242–248.

Beerling DJ, Leake JR, Long SP, Scholes JD, Ton J, Nelson PN, Bird M, Kantzas E, Taylor LL, Sarkar B *et al.* 2018. Farming with crops and rocks to address global climate, food and soil security. *Nature Plants* **4**: 392.

Bending GD, Read DJ. 1995. The structure and function of the vegetative mycelium of ectomycorrhizal plants. 5. Foraging behaviour and translocation of nutrients from exploited litter. *New Phytologist* **130**: 401–409.

Berner RA. 1997. The rise of plants and their effect on weathering and atmospheric CO_2. *Science* **276**: 544–546.

Bolou-Bi BE, Dambrine E, Angeli N, Pollier B, Nys C, Guerold F, Legout A. 2016. Magnesium isotope variations to trace liming input to terrestrial ecosystems: a case study in the Vosges Mountains. *Journal of Environmental Quality* **45**: 276–284.

Bråkenhielm S, Persson H. 1980. Vegetation dynamics in developing Scots pine stands in central Sweden. In: Persson T, ed. *Structure and function of northern coniferous forests – an ecosystem study. Ecological Bulletins* 32. Stockholm, Sweden: Swedish Natural Science Research Council (NFR), 139–152.

Bringmark L. 1980. Ion leaching through a podsol in a Scots pine stand. In: Persson T, ed. *Structure and function of northern coniferous forests – an ecosystem study. Ecological Bulletins* 32. Stockholm, Sweden: Swedish Natural Science Research Council (NFR), 341–361.

Caporaso JG, Kuczynski J, Stombaugh J, Bittinger K, Bushman FD, Costello EK, Fierer N, Pena AG, Goodrich JK, Gordon JI *et al.* 2010. QIIME allows analysis of high-throughput community sequencing data. *Nature Methods* **7**: 335–336.

Clemmensen KE, Bahr A, Ovaskainen O, Dahlberg A, Ekblad A, Wallander H, Stenlid J, Finlay RD, Wardle DA, Lindahl BD. 2013. Roots and associated fungi drive long-term carbon sequestration in boreal forest. *Science* **339**: 1615–1618.

Clemmensen KE, Durling MR, Michelsen A, Hallin S, Finlay RD, Lindahl BD. 2021. Tipping point in C storage related to mycorrhizal N recycling across the tundra-to-forest transition. *Ecology Letters* **24**: 1193–1204.

Clemmensen KE, Finlay RD, Dahlberg A, Stenlid J, Wardle DA, Lindahl BD. 2015. Carbon sequestration is related to mycorrhizal fungal community shifts during long-term succession in boreal forests. *New Phytologist* **205**: 1525–1536.

Daiogloua V, Doelmana JC, Wickeb B, Faaijc A, van Vuurena DP. 2019. Integrated assessment of biomass supply and demand in climate change mitigation scenarios. *Global Environmental Change* **54**: 88–101.

Domke GM, Oswalt SN, Walters BF, Morin RS. 2020. Tree planting has the potential to increase carbon sequestration capacity of forests in the United States. *Proceedings of the National Academy of Sciences, USA* **117**: 24649–24651.

Edgar RC. 2010. Search and clustering orders of magnitude faster than BLAST. *Bioinformatics* **26**: 2460–2461.

Ekblad A, Wallander H, Godbold DL, Cruz C, Johnson D, Baldrian P, Björk RG, Epron D, Kieliszewska-Rokicka B, Kjöller R *et al.* 2013. The production and turnover of extramatrical mycelium of ectomycorrhizal fungi in forest soils: role in carbon cycling. *Plant and Soil* **366**: 1–27.

Fahad ZA, Bolou-Bi EB, Kohler SJ, Finlay RD, Mahmood S. 2016. Fractionation and assimilation of Mg isotopes by fungi is species dependent. *Environmental Microbiology Reports* **8**: 956–965.

Finlay RD, Mahmood S, Rosenstock N, Bolou-Bi E, Köhler S, Fahad Z, Rosling A, Wallander H, Belyazid S, Bishop K *et al.* 2020. Biological weathering and its consequences at different spatial levels – from nanoscale to global scale. *Biogeosciences* **17**: 1507–1533.

Galy A, Yoffe O, Janney P, Williams R, Cloquet C, Alard O, Halicz L, Wadhwa M, Hutcheon I, Ramon E *et al.* 2003. Magnesium isotope heterogeneity of the isotopic standard SRM980 and new reference materials for magnesium-isotope-ratio measurements. *Journal of Analytical Atomic Spectroscopy* **18**: 1352–1356.

Giesler R, Petersson T, Högberg P. 2002. Phosphorus limitation in boreal forests: effects of aluminum and iron accumulation in the humus layer. *Ecosystems* **5**: 300–314.

Giesler R, Satoh F, Ilstedt U, Nordgren A. 2004. Microbially available phosphorus in boreal forests: effects of aluminium and iron in the humus layer. *Ecosystems* **7**: 208–217.

Grigal DF, Vance ED. 2000. Influence of soil organic matter on forest productivity. *New Zealand Journal of Forest Science* **30**: 169–205.

Heinonsalo J, Sun H, Santalahti M, Bäcklund K, Hari P, Pumpanen J. 2015. Evidences on the ability of mycorrhizal genus *Piloderma* to use organic nitrogen and deliver it to Scots pine. *PLoS ONE* **10**: e0131561.

Helmisaari H-S. 1995. Nutrient cycling in *Pinus sylvestris* stands in eastern Finland. *Plant and Soil* **168–169**: 327–336.

Hjelm K, Nilsson U, Johansson U, Nordin P. 2019. Effects of mechanical site preparation and slash removal on long-term productivity of conifer plantations in Sweden. *Canadian Journal of Forest Research* **49**: 1311–1319.

Högberg MN, Briones MJI, Keel SG, Metcalfe DB, Campbell C, Midwood AJ, Thornton B, Hurry V, Linder S, Näsholm T *et al.* 2010. Quantification of effects of season and nitrogen supply on tree below-ground carbon transfer to ectomycorrhizal fungi and other soil organisms in a boreal pine forest. *New Phytologist* **187**: 485–493.

Högberg P. 1997. Tansley Review No. 95. ^{15}N natural abundance in soil–plant systems. *New Phytologist* **137**: 179–203.

Ihrmark K, Bodeker ITM, Cruz-Martinez K, Friberg H, Kubartova A, Schenck J, Strid Y, Stenlid J, Brandstrom-Durling M, Clemmensen KE *et al.* 2012. New primers to amplify the fungal ITS2 region - evaluation by 454-sequencing of artificial and natural communities. *FEMS Microbiology Ecology* **82**: 666–677.

Jentschke G, Brandes B, Kuhn AJ, Schröder WH, Becker JS, Godbold DL. 2000. The mycorrhizal fungus *Paxillus involutus* transports magnesium to Norway spruce seedlings. Evidence from stable isotope labeling. *Plant and Soil* **220**: 243–246.

Jones DL, Nguyen C, Finlay RD. 2009. Carbon flow in the rhizosphere: carbon trading at the soil-root interface. *Plant and Soil* **321**: 5–33.

Jongmans AG, van Breemen N, Lundström U, van Hees PAW, Finlay RD, Srinivasan M, Unestam T, Giesler R, Melkerud P-A, Olsson M. 1997. Rock-eating fungi. *Nature* **389**: 682–683.

Kantzas EP, Martin MV, Lomas MR, Eufrasio RM, Renforth P, Lewis AL, Taylor LL, Mecure J-F, Pollitt H, Vercoulen PV *et al.* 2022. Substantial carbon drawdown potential from enhanced rock weathering in the United Kingdom. *Nature Geoscience* **15**: 382–389.

Kastner T, Matej S, Forrest M, Gingrich S, Haberl H, Hickler T, Krausmann F, Lasslop G, Niedertscheider M, Plutzar C *et al.* 2021. Land use intensification increasingly drives the spatiotemporal patterns of the global human appropriation of net primary production in the last century. *Global Change Biology* **28**: 307–322.

Kõljalg U, Nilsson RH, Abarenkov K, Tedersoo L, Taylor AFS, Bahram M, Bates ST, Bruns TD, Bengtsson-Palme J, Callaghan TM *et al.* 2013. Towards a unified paradigm for sequence-based identification of fungi. *Molecular Ecology* **22**: 5271–5277.

Law BE, Hudiburg TW, Berner LT, Kent JJ, Buotte PC, Harmon ME. 2018. Land use strategies to mitigate climate change in carbon dense temperate forests. *Proceedings of the National Academy of Sciences, USA* **115**: 3663–3668.

Leake JR, Read DJ. 2017. Mycorrhizal symbioses and pedogenesis throughout Earth's history. In: Johnson NC, Gehring K, Jansa J, eds. *Mycorrhizal mediation of soil: fertility, structure and carbon storage*. Amsterdam, the Netherlands: Elsevier, 9–33.

Lindahl BD, Kyaschenko J, Varenius K, Clemmensen KE, Dahlberg A, Karltun E, Stendahl J. 2021. A group of ectomycorrhizal fungi restricts organic matter accumulation in boreal forest. *Ecology Letters* **24**: 1341–1351.

Lindahl BD, Tunlid A. 2015. Ectomycorrhizal fungi - potential organic matter decomposers, yet not saprotrophs. *New Phytologist* **205**: 1443–1447.

Mahmood S, Finlay RD, Erland S. 1999. Effects of repeated harvesting of forest residues on the ectomycorrhizal community in a Swedish spruce forest. *New Phytologist* **142**: 577–586.

Marupakula S, Mahmood S, Clemmensen KE, Jacobson S, Högbom L, Finlay RD. 2021. Root associated fungi respond more strongly than rhizosphere soil fungi to N fertilization in a boreal forest. *Science of the Total Environment* **766**: 142597.

Marupakula S, Mahmood S, Jernberg J, Nallanchakravarthula S, Fahad ZA, Finlay RD. 2017. Bacterial microbiomes of individual ectomycorrhizal *Pinus sylvestris* roots are shaped by soil horizon and differentially sensitive to nitrogen addition. *Environmental Microbiology* **19**: 4736–4753.

Mielke LA, Ekblad A, Finlay RD, Fransson P, Lindahl BD, Clemmensen KE. 2022. Ericaceous dwarf shrubs contribute a significant but drought-sensitive fraction of soil respiration in a boreal pine forest. *Journal of Ecology* **110**: 1928–1941.

Näsholm T, Högberg P, Franklin O, Metcalfe D, Keel SG, Campbell C, Hurry V, Linder S, Högberg MN. 2013. Are ectomycorrhizal fungi alleviating or aggravating nitrogen limitation of tree growth in boreal forests? *New Phytologist* **198**: 214–221.

Nave LE, Domke GM, Hofmeister KL, Mishra U, Perry CH, Walters BF, Swanston CW. 2018. Reforestation can sequester two petagrams of carbon in US topsoils in a century. *Proceedings of the National Academy of Sciences, USA* **115**: 2776–2781.

Nguyen NH, Song Z, Bates ST, Branco S, Tedersoo L, Menke L, Schilling JS, Kennedy PG. 2016. FUNGuild: an open annotation tool for parsing fungal community datasets by ecological guild. *Fungal Ecology* **20**: 241–248.

Nicolás C, Martin-Bertelsen T, Floudas D, Bentzer J, Smits M, Johansson T, Troein C, Persson P, Tunlid A. 2018. The soil organic matter decomposition mechanisms in ectomycorrhizal fungi are tuned for liberating soil organic nitrogen. *ISME Journal* **13**: 977–988.

Nilsson RH, Tedersoo L, Ryberg M, Kristiansson E, Hartmann M, Unterseher M, Porter TM, Bengtsson-Palme J, Walker DM, de Sousa F *et al.* 2015. A comprehensive, automatically updated fungal ITS sequence dataset for reference-based chimera control in environmental sequencing efforts. *Microbes and Environments* **30**: 145–150.

Palmer L. 2021. How trees and forests reduce risks from climate change. *Nature Climate Change* **11**: 374–377.

Pan YD, Birdsey RA, Fang J, Houghton R, Kauppi PE, Kurz WA, Phillips OL, Shvidenko A, Lewis SL, Canadell JG *et al.* 2011. A large and persistent carbon sink in the world's forests. *Science* **333**: 988–993.

Perakis SS, Pett-Ridge JC. 2019. Nitrogen-fixing red alder trees tap rock-derived nutrients. *Proceedings of the National Academy of Sciences, USA* **116**: 5009–5014.

Persson T, ed. 1980. *Structure and function of northern coniferous forests – an ecosystem study. Ecological Bulletins* 32.

Pugh TAM, Lindeskog M, Smith B, Poulter B, Arneth A, Haverd V, Calle L. 2019. Role of forest regrowth in global carbon sink dynamics. *Proceedings of the National Academy of Sciences, USA* **116**: 4382–4387.

Quirk J, Andrews MY, Leake JR, Banwart SA, Beerling DJ. 2014. Ectomycorrhizal fungi and past high CO_2 atmospheres enhance mineral weathering through increased below-ground carbon-energy fluxes. *Biology Letters* **10**: 20140375.

Quirk J, Beerling DJ, Banwart SA, Kakonyi G, Romero-Gonzalez ME, Leake JR. 2012. Evolution of trees and mycorrhizal fungi intensifies silicate mineral weathering. *Biology Letters* **8**: 1006–1011.

Rineau F, Shah F, Smits M, Persson P, Johansson T, Carleer R, Troein C, Tunlid A. 2013. Carbon availability triggers the decomposition of plant litter and assimilation of nitrogen by an ectomycorrhizal fungus. *ISME Journal* **7**: 2010–2022.

Rognes T, Flouri T, Nichols B, Quince C, Mahé F. 2016. VSEARCH: a versatile open-source tool for metagenomics. *PeerJ* **4**: e2584.

Rosling A, Landeweert R, Lindahl BD, Larsson K-H, Kuyper TW, Taylor AFS, Finlay RD. 2003. Vertical distribution of ectomycorrhizal fungal taxa in a podzol profile determined by morphotyping and genetic verification. *New Phytologist* **159**: 775–783.

Rosling A, Lindahl BD, Finlay RD. 2004. Carbon allocation to ectomycorrhizal roots and mycelium colonising different mineral substrates. *New Phytologist* **162**: 795–802.

Schloss PD, Westcott SL, Ryabin T, Hall JR, Hartmann M, Hollister EB, Lesniewski RA, Oakley BB, Parks DH, Robinson CJ *et al.* 2009. Introducing MOTHUR: open-source, platform-independent, community-supported software for describing and comparing microbial communities. *Applied and Environmental Microbiology* **75**: 7537–7541.

See CR, Keller AB, Hobbie SE, Kennedy PG, Weber PK, Pett-Ridge J. 2022. Hyphae move matter and microbes to mineral microsites: integrating the hyphosphere into conceptual models of soil organic matter stabilization. *Global Change Biology* **28**: 2527–2540.

Shah F, Nicolás C, Bentzer J, Ellström M, Smits M, Rineau F, Canbäck B, Floudas D, Carleer R, Lackner G *et al.* 2016. Ectomycorrhizal fungi decompose soil organic matter using oxidative mechanisms adapted from saprotrophic ancestors. *New Phytologist* **209**: 1705–1719.

Smits MM, Bonneville S, Benning LG, Banwart SA, Leake JR. 2012. Plant-driven weathering of apatite – the role of an ectomycorrhizal fungus. *Geobiology* **10**: 445–456.

Sokol NW, Bradford MA. 2019. Microbial formation of stable soil carbon is more efficient from belowground than aboveground input. *Nature Geoscience* **12**: 46–53.

Taylor LL, Quirk J, Thorley RMS, Kharecha PA, Hansen J, Ridgwell A, Lomas MR, Banwart SA, Beerling DJ. 2016. Enhanced weathering strategies for stabilizing climate and averting ocean acidification. *Nature Climate Change* **6**: 402–408.

Van Hees PAW, Rosling A, Essén S, Godbold DL, Jones DL, Finlay RD. 2005. The carbon we do not see – the impact of low molecular weight compounds on carbon dynamics and respiration in forest soils: a review. *Soil Biology and Biochemistry* **37**: 1–13.

Vicca S, Goll DS, Hagens M, Hartmann J, Janssens IA, Neubeck A, Peñuelas J, Poblador S, Rijnders J, Sardans J *et al.* 2022. Is the climate change mitigation effect of enhanced silicate weathering governed by biological processes? *Global Change Biology* **28**: 711–726.

Vincent AG, Schleucher J, Giesler R, Wardle DA. 2022. Soil phosphorus forms show only minor changes across a 5000-year-old boreal wildfire chronosequence. *Biogeochemistry* **159**: 15–32.

Vincent AG, Schleucher J, Gröbner G, Vestergren J, Persson P, Jansson M, Giesler R. 2012. Changes in organic phosphorus composition in boreal forest humus soils: the role of iron and aluminium. *Biogeochemistry* **108**: 485–499.

Wallander H, Mahmood S, Hagerberg D, Johansson L, Pallon J. 2003. Elemental composition of ectomycorrhizal mycelia identified by PCR–RFLP analysis and grown in contact with apatite or wood ash in forest soil. *FEMS Microbiology Ecology* **44**: 57–65.

White T, Bruns T, Lee S, Taylor J. 1990. Amplification and direct sequencing of fungal ribosomal RNA genes for phylogenetics. In: Innis MA, Gelfland DH, Sninsky JJ, White TJ, eds. *PCR protocols: a guide to methods and applications*. San Diego, CA, USA: Academic Press, 315–322.

Zak DR, Pellitier PT, Argiroff WA, Castillo B, James TY, Nave LE, Averill C, Beidler KV, Bhatnagar J, Blesh J *et al.* 2019. Exploring the role of ectomycorrhizal fungi in soil carbon dynamics. *New Phytologist* **223**: 33–39.

Supporting Information

Additional Supporting Information may be found online in the Supporting Information section at the end of the article.

Fig. S1 Effects of organic matter availability on mycelial biomass and $\delta^{15}N$ signatures of plants and soils.

Fig. S2 Positive effects of increasing organic matter availability on mycelial biomass and the subsequent positive effect on acquisition of Ca, K and Mg.

Fig. S3 Variation in the $\delta^{26}Mg$ isotopic ratio of soil solution in organic and mineral soil horizons in relation to soil solution content of different elements.

Fig. S4 Fungal community composition of organic and mineral horizon soils and mycelial in-growth mesh bags.

Fig. S5 Influence of different availability of organic matter on fungal taxa, saprotrophic and ectomycorrhizal guild interactions, and the role of ectomycorrhizal fungi in base cation and P mobilisation in mineral B horizon soil.

Fig. S6 Effects of changing soil organic matter availability on relative abundance of fungal taxa and functional guilds in in-growth mesh bags.

Fig. S7 Relationships between elemental contents of plants and the abundance of ectomycorrhizal and saprotrophic guilds in soil.

Fig. S8 Relationships between pH of soil solution and the relative abundance of ectomycorrhizal and saprotrophic guilds in soil.

Methods S1 Harvesting of microcosms; PCR amplification conditions.

Table S1 Elemental composition of soil samples from each of the organic (O), eluvial (E) and illuvial (B) horizons in a boreal forest podzol profile.

Table S2 Total and proportional (%) distribution of solubilised elements in plant biomass, mycelial biomass and soil solution in microcosms containing *Pinus sylvestris* plants growing in a reconstructed boreal forest podzol.

Please note: Wiley is not responsible for the content or functionality of any Supporting Information supplied by the authors. Any queries (other than missing material) should be directed to the *New Phytologist* Central Office.